Colloidal Surfactants

DOI: 10.1002/anie.201208293

Janus Micelles as Effective Supracolloidal Dispersants for Carbon Nanotubes**

André H. Gröschel, Tina I. Löbling, Petar D. Petrov, Markus Müllner, Christian Kuttner, Florian Wieberger, and Axel H. E. Müller**

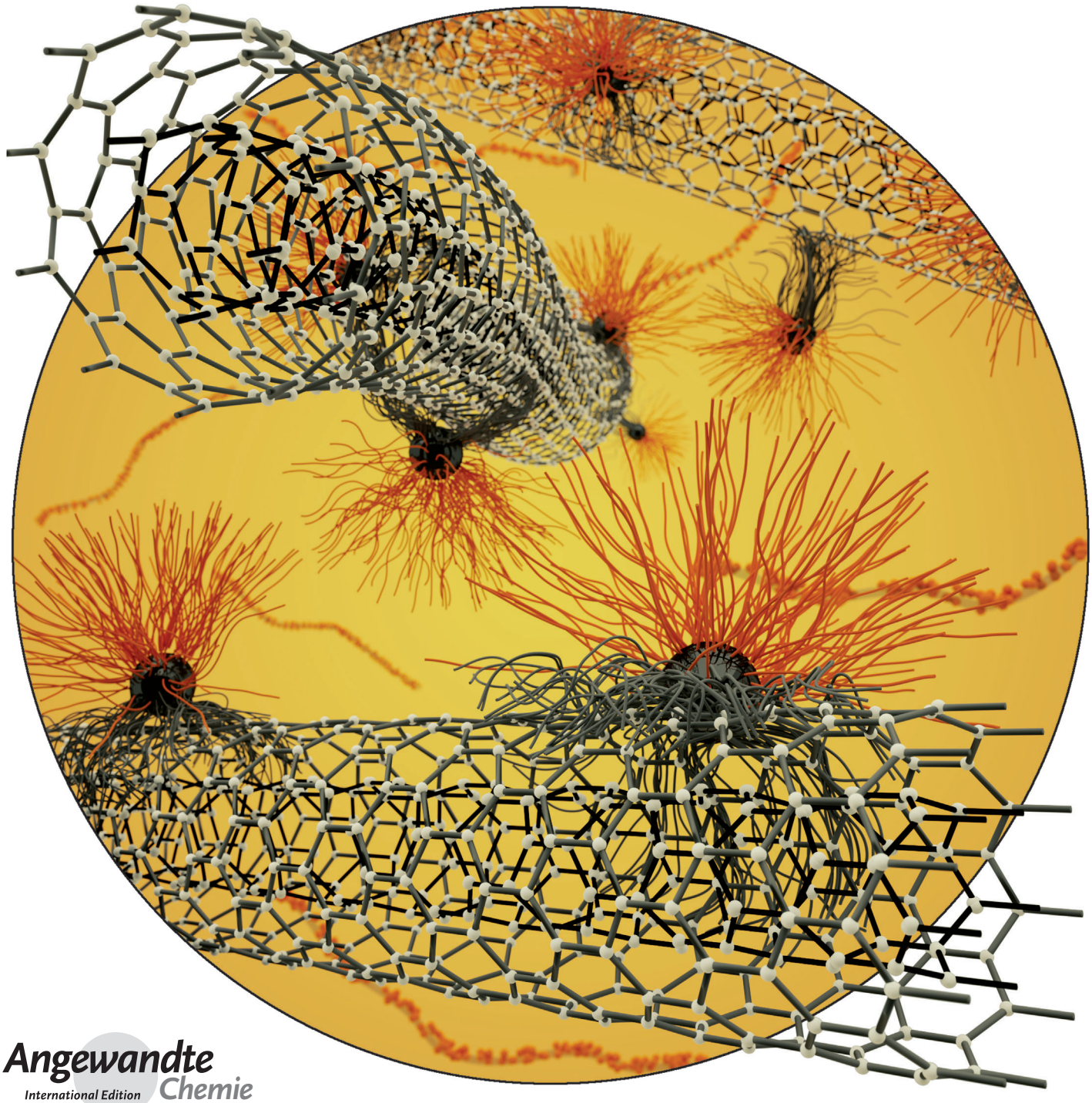

Carbon nanotubes (CNTs) are undoubtedly exceptional materials in nanotechnology and materials science.[1,2] Their outstanding strength, robustness, and electrical and thermal conductivity make them very attractive components for numerous innovative composites.[3–6] A uniform distribution of CNTs in the target medium, for example, solvent or polymer matrix, is often required to fully harness the desired properties and to enhance CNT processability. However, the high cohesion energy (π stacking) combined with a low solubility parameter promotes extreme bundling of CNTs to minimize the interactions with the surrounding medium.[6,7] It is therefore necessary to stabilize each CNT with a surface coating either by covalent attachment (grafting to/from) or physisorption of polymers.[8–14] Covalent attachment provides very good stabilization, yet this "anchoring" also interrupts the conjugated π system thus interfering with the CNT's properties. Physisorbed moieties are better suited as they show excellent stabilization, while maintaining the structural integrity of the CNTs. Noncovalent dispersants range from pure organic compounds to surfactants[15–17] and block copolymers,[18–22] and recently, even block copolymer micelles.[23,24] Organic solvents have the disadvantage that the CNTs cannot be transferred into other media without coagulation and precipitation. Surfactants and amphiphilic block copolymers can be tailored to match any solvent, but often require a high dispersant-to-CNT weight ratio to form stable dispersions.[18] In comparison, block copolymer micelles have similar stabilizing properties, while requiring lower dispersant/CNT ratios.[23] These developments mirror that the trend is clearly shifting towards more sophisticated dispersants unifying strong adsorption to the CNTs and enhanced stabilization, preferably in many different media.

[*] Dipl.-Chem. A. H. Gröschel,[+] M. Sc. T. I. Löbling, Dr. M. Müllner,[++] Prof. Dr. A. H. E. Müller[+++]
Makromolekulare Chemie II, Universität Bayreuth
95440 Bayreuth (Germany)
E-mail: andre.groschel@aalto.fi
axel.mueller@uni-mainz.de
Dr. F. Wieberger
Makromolekulare Chemie I, Universität Bayreuth
95440 Bayreuth (Germany)
Dipl.-Chem. C. Kuttner
Physikalische Chemie II, Universität Bayreuth
95440 Bayreuth (Germany)
Prof. Dr. P. D. Petrov
Institute of Polymers, Bulgarian Academy of Sciences
Sofia 1113 (Bulgaria)
[+] Current address: Molecular Materials, Department of Applied Physics
Aalto University (Finland)
[++] Current address: Department of Chemical & Biomolecular Engineering, University of Melbourne (Australia)
[+++] Current address: Institut für Organische Chemie
Johannes-Gutenberg-Universität Mainz (Germany)
[**] This work was supported by the Deutsche Forschungsgemeinschaft within SFB 840 (TP A1) and Mu896/39-1. We thank Prof. Andreas Fery for his support in analyzing the JM-MWNT interaction.
Supporting information for this article is available on the WWW under http://dx.doi.org/10.1002/anie.201208293.

Janus particles of various topologies[25–29] have a strong affinity towards interfaces,[30–32] outstanding performance as "giant surfactants" in emulsion polymerization, and as compatibilizers in polymer blends.[33,34] The strong interfacial affinity originates from the Pickering effect[35] and the two strictly phase-separated corona patches.

Herein, we demonstrate that polymer-based Janus micelles (JMs) facilitate the dispersion of multi-walled carbon nanotubes (MWNTs) in a variety of solvents, including water. JMs selectively adsorb to the MWNTs with a π-stacking hemisphere, while stabilizing the formed supracolloidal hybrid in the chosen medium through steric repulsion with a solvophilic hemisphere (Scheme 1). The non-invasive physisorption preserves the conjugated structure of the MWNTs, essential for maintaining its properties.

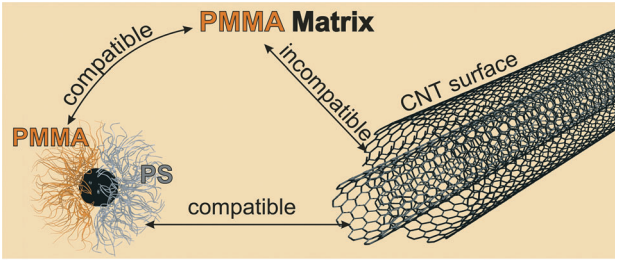

Scheme 1. Janus micelles functioning as compatibilizers between MWNTs and a polymer matrix.

We recently developed a large-scale approach allowing the functional design of nanoscale JMs[36,37] with respect to size, corona chemistry, and Janus balance (JB), all properties which are decisive for MWNT dispersion as summarized in Table 1. The overall size of the JMs can be tailored from 20–100 nm, thus matching the outer diameter of MWNTs, typically in the range of 10–100 nm. Larger particles (over 100 nm) may attach to several tubes causing network formation and precipitation. Matching sizes are essential to enhance particle–particle interaction as recently demonstrated for a biomimetic composite, in which a "Janus-like" protein, hydrophobin, facilitates extremely strong supramolecular interaction between nanofibrillated cellulose and graphene.[38] In our case, the tasks of the corona hemispheres can be tailored to meet application needs, simply by choosing the proper ABC triblock terpolymer. Beyond that, we systematically vary the rarely addressed Janus balance, that is, the size ratio of both corona patches, from dominant adsorbant to dominant stabilizer and show its critical impact on the effectiveness of the dispersant.

The experimental approach to JM/MWNT hybrids is straightforward and will be shown for polystyrene-*block*-polybutadiene-*block*-poly(methyl methacrylate) (PS-PB-PMMA; SBM) JMs with a cross-linked PB core, a dominant PS, and a minor PMMA patch ($JB_{PS} = 68\,\%$).

Pristine, untreated MWNTs were dispersed in acetone together with SBM1 JMs at a weight ratio of 50:50 *w*/*w* to yield a final MWNT concentration of 0.05 $g\,L^{-1}$. Acetone is a good solvent for M, a near-theta solvent (that is, the polymer exists as a statistical coil and is at the edge of solubility) for S,

Table 1: Characteristics of used Janus Micelles.

Code	Polymer[a]	R_h [nm][b]	d_{core} [nm][c]	JB_{PS} [%][d]
SBM1	$S_{610}B_{640}M_{290}^{127}$	35 ± 3	31 ± 5	68
SBM2	$S_{340}B_{330}M_{360}^{90}$	25 ± 4	22 ± 4	48
SBM3	$S_{280}B_{330}M_{430}^{90}$	27 ± 3	21 ± 3	39
SBT	$S_{580}B_{120}T_{470}^{134}$	29 ± 2	10 ± 2	55
SBV	$S_{360}B_{380}V_{590}^{120}$	29 ± 7	14 ± 3	38

[a] Subscript denotes the number-average degree of polymerization, DP_n, and superscript the molecular weight in kg mol^{-1}. [b] Hydrodynamic radius in THF at $c = 1$ g L^{-1}. [c] Average diameter from TEM image analysis of 250 cores.[41] [d] Janus balance, $JB_{PS} = DP_{n,PS}/(DP_{n,PS}+DP_{n,C})$ with C = PMMA, PtBMA, or P2VP.

and a non-solvent for the MWNTs. Thus, the MWNTs entangle into strongly interacting bundles (sedimentation), whereas the solvophobic S-patches cause clustering of JM (Figure 1 A). This mixture was sonicated to disassemble the MWNTs and the JM clusters. After treatment, re-assembly results in the adsorption of JMs onto the MWNTs surface to minimize energetically unfavorable solvent/solvophobic

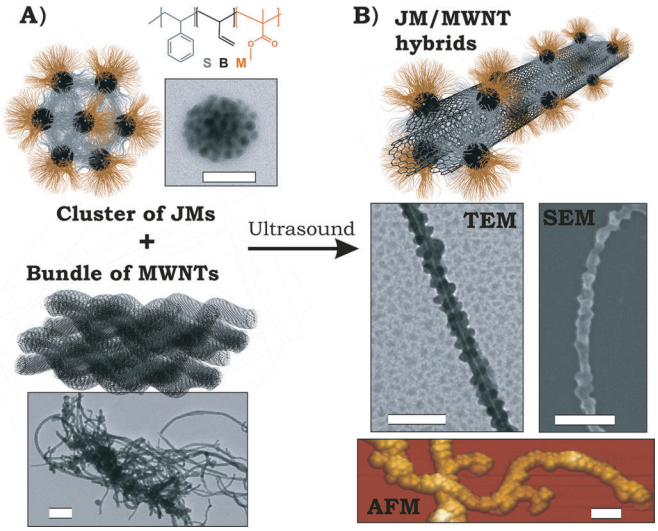

Figure 1. General preparation procedure. A) Schematic representation and TEM images of starting materials in acetone. B) Supracolloidal re-assembly (scale bars are 200 nm).

interfaces. Thereby, the PMMA-patches provide steric repulsion, suppressing rebundling of the MWNTs and promote the formation of a stable dispersion. A dense coating of JMs on to the MWNTs is evident from the large number of spherical particles on the surface as seen by transmission and scanning electron microscopy (TEM, SEM) and atomic force microscopy (AFM, Figure 1 B). Raman spectroscopy shows that the CNT surface is not affected by this supracolloidal attachment and in IR measurements both materials contribute to the spectrum (Figure S1–3 in the Supporting Information).

Surprisingly, the JMs selectively attach to the MWNTs instead of re-assembling with each other, irrespective of JM concentration or Janus balance. At a JM/MWNT ratio of 33:66 *w*/*w*, the JMs fully attach to the MWNTs and no clusters or residual JMs can be identified (Figure 2 A). Dense packing

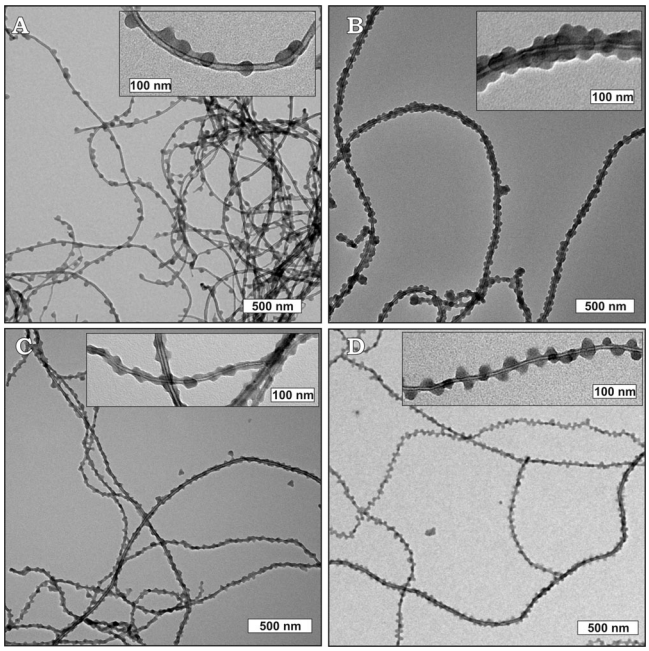

Figure 2. Adsorption pattern of SBM1 JMs to MWCNTs in acetone at A) 80:20 *w*/*w* and B) at 50:50 *w*/*w*, C) of SBM2, and D) of SBM3 both 50:50 *w*/*w*.

is not observed at this stage, because there is still enough space for the JMs to distribute evenly along the MWNT surface. At a ratio of 50:50 *w*/*w*, SBM1 forms a dense multilayer packing, but still no residual JMs are found (Figure 2 B). However, an excess of JMs (90:10 *w*/*w*) results in quantitative coverage, multilayer formation, and growth of JM clusters from the surface (Figure S4). Only then, does a fraction of the JMs re-assemble into the former raspberry-like shape. We attribute the strong and selective affinity of the JMs towards the solvent/MWNT-interface to 1) the Pickering effect,[35] 2) π stacking of the polystyrene hemisphere facing towards the sp^2-hybridized carbon surface, but mostly, to 3) minimization of unfavorable interfacial energies. In good solvents, such as THF (or less polar), JMs do not attach to the MWNTs but are evenly scattered on the TEM grid as the driving force for surface-energy minimization is greatly reduced. Repeatedly changing the solvent conditions, allows reversible switching between the adsorbed (in acetone) and desorbed state (in THF), underlining the supracolloidal nature of the JM/MWNT interaction (Figure S5).

In recent work, we and others showed that the Janus balance is a key element determining the aggregation behavior of JMs in selective solvents.[36,39,40] Herein, we demonstrate its fundamental influence on the quantity of adsorbed JMs on a set of SBM JMs ranging from dominant adsorbing (SBM1, $JB_{PS} = 68\,\%$) to equal-sized (SBM2, $JB_{PS} = 48\,\%$), to dominant stabilizing patch (SBM3, $JB_{PS} = 39\,\%$). The adsorption behavior in acetone is visualized qualitatively in TEM (Figure 2 B–D, S4–7) and monitored quantitatively by thermogravimetric analysis (TGA) (Figure 3, S8, S9). As long as the surface is not saturated (less than 50:50 *w*/*w*), we observe quantitative adsorption corroborated by the linear relationship in Figure 3 (and also by the absence of residual

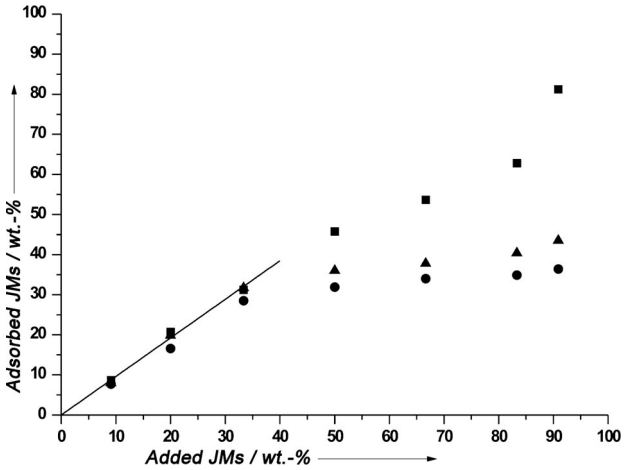

Figure 3. Adsorption efficiency of SBM1–3 JMs relative to their Janus balance as determined by thermogravimetric analysis. ■: SBM1, $JB_{PS} = 69\%$, ▲: SBM2, $JB_{PS} = 48\%$, ●: SBM3, $JB_{PS} = 39\%$, ——: linear region.

JMs in Figure 2B–D). At a constant weight ratio of 66:33 *w*/*w*, the amount of adsorbed JMs decreases from SBM1 to SBM3. SBM1 has the largest adsorbing S patch and the smallest repulsive PMMA corona, both factors promoting dense packing. After adsorption, the "sticky" S patch attracts other JMs inducing a cascade effect as every newly attached JM generates an additional hydrophobic surface. Even at very high JM content (83:17 *w*/*w*), we determine almost quantitative adsorption by TGA (ca. 70 wt%) realized by multilayer coating and cluster growth from the MWNT surface (shown by TEM, Figure S4, S8, S9). SBM2 on the other hand, displays an adsorption limit at approximately 45 wt%, reached at 50:50 *w*/*w*, which is shown by a less-dense packing as compared to SBM1 (Figure 2C). The larger stabilizing PMMA corona occupies more volume and blocks surface area for other JMs. These effects become more distinct for SBM3 (Figure 2D). In this case, the surface uptake reaches saturation at about 35 wt% as the PMMA corona requires too much space for all the JMs to be accommodated. In the TEM image the space between the particles appears to be empty, but it is occupied by poly(methyl methacrylate) (PMMA; not visible owing to e-beam degradation) and therefore not accessible for other JMs. Repulsive interactions of the solvated PMMA-corona prevent complete coverage. In both TEM and SEM, JMs are shown to be evenly spaced on the MWNT surface, reminiscent of helical packing (Figure 2D, S7). The JM–JM interparticle spacing is defined by the excluded volume of the PMMA corona. The helical wrapping of CNTs is not uncommon and has been reported for several polymers.[11]

The striking advantage of JMs is the possibility to combine and spatially divide different chemical environments within one single particle. We designed several JMs with one patch, matching the demands of increasingly polar solvents, while continuing to use the PS patch that had already demonstrated its extraordinary affinity towards MWNTs. We first exchange the PMMA-patch (which aids blending with poly(styrene-*co*-acrylonitrile) or PMMA) for poly(*tert*-butyl methacrylate) (P*t*BMA; T), which is stable in ethanol (Figure 4A). When cast from ethanol, PS-*b*-PB-*b*-P*t*BMA (SBT) JMs are only visible as regularly spaced small black dots on the MWNTs surrounded by a dark gray coating (S, selectively stained with RuO_4). PS-*b*-PB-*b*-P2VP (SBV) JMs with a pH-responsive poly(2-vinylpyridine) (P2VP; V) patch

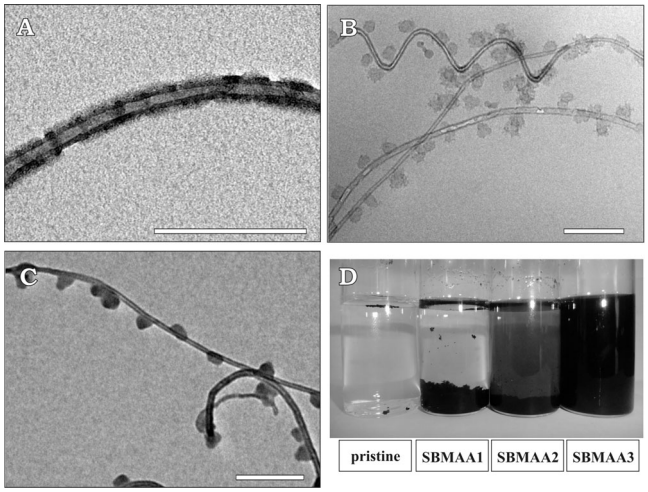

Figure 4. JM/MWNT hybrids (50:50 *w*/*w*) in protic solvents. A) SBT JMs in ethanol, B) SBV JMs in water at pH 3 (cryo-TEM), and C) SBMAA3 JMs in water at pH 10. D) MWNT dispersions in water at pH 10: pristine, stabilized by SBMAA1, SBMAA2, and SBMAA3 (scale bars are 200 nm).

allow stabilization of MWNTs in acidic water. Cryogenic TEM imaging of samples in water at pH 3 gives a clear picture of the JM distribution around the MWNTs and rules out drying artifacts (Figure 4B). P2VP is an attractive functional corona that allows the entire supracolloidal hybrid to undergo reversible precipitation/redispersion cycles with a sharp transition at pH 4 and it can also coordinate metal anions (e.g. $AuCl_4^-$, TiO_2^{2-}). JMs with a poly(methacrylic acid) (MAA) patch (SBMAA, obtained by hydrolysis of SBM),[41] form stable dispersions in neutral and basic water (Figure 4C). This hybrid shows a precipitation/redispersion transition at $pH \approx 5$ and PMAA can coordinate metal cations (e.g. Ag^+, Cd^{2+}). Surprisingly, the stability of the SBMAA/MWNT hybrids follows an inverse trend to the adsorbed mass of JMs and increases from SBMAA1 to SBMAA3 (Figure 4D). Coating with SBMAA1 ($JB_{PS} = 68\%$) induces sedimentation as a result of insufficient stabilization by the small MAA-patch. Stabilization increases for SBMAA2 and peaks for SBMAA3 ($JB_{PS} = 39\%$), clearly demonstrating that not the amount of attached JMs is decisive for stability, but rather the contribution of each JM to hybrid stabilization, that is, greatest stability is obtained with a Janus balance in favor of the stabilizing MAA-patch.

In conclusion, we demonstrated that Janus micelles are well suited as supracolloidal dispersants for carbon nanotubes. They exhibit amphiphilic character and have tunable surface patches, their supracolloidal attachment to CNTs preserves the CNTs properties, and low dispersant-to-tube weight ratios (10:90 *w*/*w*) are sufficient for stabilization. In

the dried state, the JMs act as a glue for the CNTs and the hybrid material approaches the bulk density of the glassy polymers ($\rho_{hybrid} \approx 1.15$–$1.50\ g\,cm^{-3}$), making handling safer and dosing easier. In contrast, pristine disentangled CNTs have a very low density and when dry are easily blown into the air. The quantitative coating allows precipitation, drying, long-term storage, and redispersion in any medium, matching the stabilizing corona. The Janus balance determines the quantity of adsorbed JMs and thus controls adsorption patterns ranging from multilayered to helical. The direct visualization of these adsorption patterns should aid the design of future CNT dispersants. We are currently investigating a number of other stabilizing patches, such as pH- and temperature-responsive poly(2-(dimethylamino)ethyl methacrylate), degradable poly(ε-caprolactone), or biocompatible poly(ethylene oxide).

Received: October 15, 2012
Revised: December 19, 2012
Published online: February 20, 2013

Keywords: colloids · dispersants · Janus particles · carbon nanotubes · self-assembly

[1] R. H. Baughman, A. A. Zakhidov, W. A. de Heer, *Science* **2002**, *297*, 787 – 792.
[2] G. Sahoo, S. Rana, J. W. Cho, L. Li, S. H. Chan, *Prog. Polym. Sci.* **2010**, *35*, 837 – 867.
[3] S. J. Kang, C. Kocabas, T. Ozel, M. Shim, N. Pimparkar, M. A. Alam, S. V. Rotkin, J. A. Rogers, *Nat. Nanotechnol.* **2007**, *2*, 230 – 236.
[4] Z. Han, A. Fina, *Prog. Polym. Sci.* **2011**, *36*, 914 – 944.
[5] Z. Spitalsky, D. Tasis, K. Papagelis, C. Galiotis, *Prog. Polym. Sci.* **2010**, *35*, 357 – 401.
[6] L. Hu, D. S. Hecht, G. Grüner, *Chem. Rev.* **2010**, *110*, 5790 – 5844.
[7] E. Nativ-Roth, R. Shvartzman-Cohen, C. Bounioux, M. Florent, D. Zhang, I. Szleifer, R. Yerushalmi-Rozen, *Macromolecules* **2007**, *40*, 3676 – 3685.
[8] N. Roy, R. Sengupta, A. K. Bhowmick, *Prog. Polym. Sci.* **2012**, *37*, 781 – 819.
[9] T. Akasaka, F. Wudl, S. Nagase, *Chemistry of Nanocarbons*, Wiley, Hoboken, **2010**, pp. 1 – 48.
[10] D. Tasis, N. Tagmatarchis, A. Bianco, M. Prato, *Chem. Rev.* **2006**, *106*, 1105 – 1136.
[11] A. Hirsch, *Angew. Chem.* **2002**, *114*, 1933 – 1939; *Angew. Chem. Int. Ed.* **2002**, *41*, 1853 – 1859.
[12] D. Tasis, N. Tagmatarchis, V. Georgakilas, M. Prato, *Chem. Eur. J.* **2003**, *9*, 4000 – 4008.
[13] N. Karousis, N. Tagmatarchis, D. Tasis, *Chem. Rev.* **2010**, *110*, 5366 – 5397.
[14] J.-M. Thomassin, D. Vuluga, M. Alexandre, C. Jérôme, I. Molenberg, I. Huynen, C. Detrembleur, *Polymer* **2012**, *53*, 169 – 174.
[15] M. R. Diehl, S. N. Yaliraki, R. A. Beckman, M. Barahona, J. R. Heath, *Angew. Chem.* **2002**, *114*, 363 – 366; *Angew. Chem. Int. Ed.* **2002**, *41*, 353 – 356.
[16] C. A. Furtado, U. J. Kim, H. R. Gutierrez, L. Pan, E. C. Dickey, P. C. Eklund, *J. Am. Chem. Soc.* **2004**, *126*, 6095 – 6105.
[17] K. K. Kim, S. M. Yoon, J. Y. Choi, J. Lee, B. K. Kim, J. M. Kim, J. H. Lee, U. Paik, M. H. Park, C. W. Yang, K. H. An, Y. Chung, Y. H. Lee, *Adv. Funct. Mater.* **2007**, *17*, 1775 – 1783.
[18] V. C. Moore, M. S. Strano, E. H. Haroz, R. H. Hauge, R. E. Smalley, J. Schmidt, Y. Talmon, *Nano Lett.* **2003**, *3*, 1379 – 1382.
[19] N. Sluzarenko, B. Heurtefeu, M. Maugey, C. Zakri, P. Poulin, S. Lecommandoux, *Carbon* **2006**, *44*, 3207 – 3212.
[20] J. Zou, L. Liu, H. Chen, S. I. Khondaker, R. D. McCullough, Q. Huo, L. Zhai, *Adv. Mater.* **2008**, *20*, 2055 – 2060.
[21] V. A. Sinani, M. K. Gheith, A. A. Yaroslavov, A. A. Rakhnyanskaya, K. Sun, A. A. Mamedov, J. P. Wicksted, N. A. Kotov, *J. Am. Chem. Soc.* **2005**, *127*, 3463 – 3472.
[22] S. Soll, M. Antonietti, J. Yuan, *ACS Macro Lett.* **2012**, *1*, 84 – 87.
[23] H.-I. Shin, B. G. Min, W. Jeong, C. Park, *Macromol. Rapid Commun.* **2005**, *26*, 1451 – 1457.
[24] P. D. Petrov, G. L. Georgiev, A. H. E. Müller, *Polymer* **2012**, *53*, 5502 – 5506.
[25] R. Erhardt, A. Böker, H. Zettl, H. Kaya, W. Pyckhout-Hintzen, G. Krausch, V. Abetz, A. H. E. Müller, *Macromolecules* **2001**, *34*, 1069 – 1075.
[26] A. Walther, M. Drechsler, S. Rosenfeldt, L. Harnau, M. Ballauff, V. Abetz, A. H. E. Müller, *J. Am. Chem. Soc.* **2009**, *131*, 4720 – 4728.
[27] F. Wurm, A. F. M. Kilbinger, *Angew. Chem.* **2009**, *121*, 8564 – 8574; *Angew. Chem. Int. Ed.* **2009**, *48*, 8412 – 8421.
[28] D. Hirsemann, S. Shylesh, R. A. De Souza, B. Diar-Bakerly, B. Biersack, D. N. Mueller, M. Martin, R. Schobert, J. Breu, *Angew. Chem.* **2012**, *124*, 1376 – 1380; *Angew. Chem. Int. Ed.* **2012**, *51*, 1348 – 1352.
[29] A. Walther, A. H. E. Müller, *Soft Matter* **2008**, *4*, 663 – 668.
[30] A. Walther, X. André, M. Drechsler, V. Abetz, A. H. E. Müller, *J. Am. Chem. Soc.* **2007**, *129*, 6187 – 6198.
[31] N. Glaser, D. J. Adams, A. Böker, G. Krausch, *Langmuir* **2006**, *22*, 5227 – 5229.
[32] T. M. Ruhland, A. H. Gröschel, A. Walther, A. H. E. Müller, *Langmuir* **2011**, *27*, 9807 – 9814.
[33] A. Walther, M. Hoffmann, A. H. E. Müller, *Angew. Chem.* **2008**, *120*, 723 – 726; *Angew. Chem. Int. Ed.* **2008**, *47*, 711 – 714.
[34] A. Walther, K. Matussek, A. H. E. Müller, *ACS Nano* **2008**, *2*, 1167 – 1178.
[35] B. P. Binks, P. D. I. Fletcher, *Langmuir* **2001**, *17*, 4708 – 4710.
[36] A. H. Gröschel, F. H. Schacher, H. Schmalz, O. V. Borisov, E. B. Zhulina, A. Walther, A. H. E. Müller, *Nat. Commun.* **2012**, *3*, 710.
[37] A. H. Gröschel, A. Walther, T. I. Löbling, J. Schmelz, A. Hanisch, H. Schmalz, A. H. E. Müller, *J. Am. Chem. Soc.* **2012**, *134*, 13850 – 13860.
[38] P. Laaksonen, A. Walther, J.-M. Malho, M. Kainlauri, O. Ikkala, M. B. Linder, *Angew. Chem.* **2011**, *123*, 8847 – 8850; *Angew. Chem. Int. Ed.* **2011**, *50*, 8688 – 8691.
[39] S. Jiang, S. Granick, *J. Chem. Phys.* **2007**, *127*, 161102 – 161104.
[40] S. Jiang, S. Granick, *Langmuir* **2008**, *24*, 2438 – 2445.
[41] R. Erhardt, M. Zhang, A. Böker, H. Zettl, C. Abetz, P. Frederik, G. Krausch, V. Abetz, A. H. E. Müller, *J. Am. Chem. Soc.* **2003**, *125*, 3260 – 3267.

